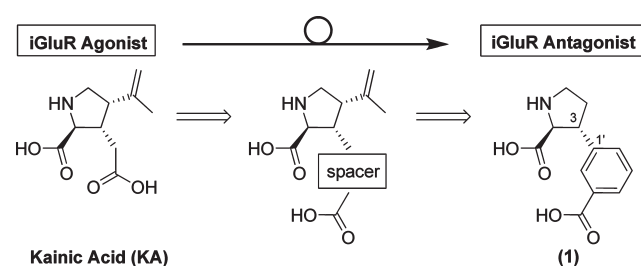


Discovery of a New Class of Ionotropic Glutamate Receptor Antagonists by the Rational Design of (2*S*,3*R*)-3-(3-Carboxyphenyl)-pyrrolidine-2-carboxylic Acid

Ann M. Larsen,[†] Raminta Venskutonytė,^{†,‡} Elena Antón Valadés,[‡] Birgitte Nielsen,[†] Darryl S. Pickering,[‡] and Lennart Bunch^{*,†}

[†]Department of Medicinal Chemistry, Faculty of Pharmaceutical Sciences, University of Copenhagen, Universitetsparken 2, DK-2100 Copenhagen, Denmark, and [‡]Department of Pharmacology and Pharmacotherapy, Faculty of Pharmaceutical Sciences, University of Copenhagen, Universitetsparken 2, DK-2100 Copenhagen, Denmark

Abstract



The kainic acid (KA) receptors belong to the class of glutamate (Glu) receptors in the brain and constitute a promising target for the treatment of neurological and/or psychiatric diseases such as schizophrenia, major depression, and epilepsy. Five KA subtypes have been identified and named GluK1–5. In this article, we present the discovery of (2*S*,3*R*)-3-(3-carboxyphenyl)-pyrrolidine-2-carboxylic acid (**1**) based on a rational design process. Target compound **1** was synthesized by a stereoselective strategy in 10 steps from commercially available starting materials. Binding affinities of **1** at native ionotropic Glu receptors were determined to be in the micromolar range (AMPA, 51 μM ; KA, 22 μM ; NMDA 6 μM), with the highest affinity for cloned homomeric KA receptor subtypes GluK1,3 (3.0 and 8.1 μM , respectively). Functional characterization of **1** by two electrode voltage clamp (TEVC) electrophysiology at a nondesensitizing mutant of GluK1 showed full competitive antagonistic behavior with a K_b of 11.4 μM .

Keywords: Glutamate receptors, kainic acid receptors, antagonist, rational design

Introduction

In the mammalian central nervous system (CNS), (*S*)-glutamate (Glu) functions as the major excitatory neurotransmitter. Once released from the presynaptic neuron into the glutamatergic synapse, Glu activates a number of pre- and postsynaptic glutamate

receptors. On the basis of pharmacological profile and ligand selectivity studies, the Glu receptors have been grouped into two main classes: the fast-acting *ionotropic receptors* (iGluRs) (1, 2) and the G-protein coupled *metabotropic receptors* (mGluRs), which produce a much slower signal transduction through second messenger systems (3). Within the class of iGluRs, three subgroups have been established on the basis of ligand affinity studies: the AMPA (subunits GluA1–4), kainic acid (KA) (subunits GluK1–5), and NMDA receptors (subunits GluN1, GluN2A–D, and GluN3A,B). Likewise for the mGluRs, three subgroups have been defined and named group I (subunits mGluR1,5), group II (subunits mGluR2,3) and group III (subunits mGluR4,6–8). The uptake of Glu is carried out by the action of the *excitatory amino acid transporters* (EAATs) and plays an important role in the termination of the neuronal signaling process and in keeping the concentration of Glu below neurotoxic levels.

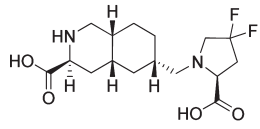
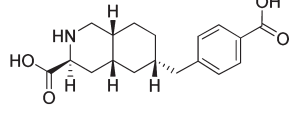
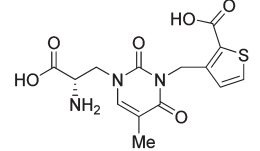
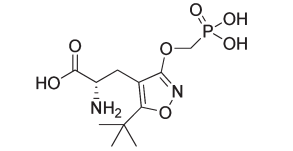
In order to understand the physiological role of the different Glu receptor subunits, the development of subtype selective ligands is a key strategy. Such pharmacological tools, agonists, antagonists, and positive/negative modulators may be used for the functional studies of isolated receptors, neuronal tissue, and *in vivo*. With a focus on the KA receptors, they have been suggested to be involved in modulating synaptic transmission and plasticity (4, 5), particularly in the hippocampal region (6, 7). Thus KA receptors may be promising targets in the treatment of schizophrenia, major depression, epilepsy, and neurodegeneration (8). However, despite an extensive effort only truly subtype selective antagonists for the GluK1 subtype have been reported (9). In this article, we present the discovery of **1** as the lead structure for a new class of selective iGluR antagonists, which due to its vast substitution options holds potential for future development into new subtype selective KA receptor antagonists.

Received Date: October 7, 2010

Accepted Date: November 4, 2010

Published on Web Date: November 12, 2010

Table 1. Selected Examples of Competitive iGluR Antagonists Which Comprise an α -Amino Acid Moiety and the Distance from the α -Carbon to the Carbon of the Distal Carboxylic Acid in [Å]

	
LY 466195	LY 382884
	
UBP310	(S)-ATPO

	dist [Å]	subtype, PDB code	ligand class
Glu	3.15	GluK1, 1TFX	agonist
KA	3.35	GluK2, 1TT1	agonist
ATPO	5.31	GluK1, 1VSO	antagonist
UBP310	7.55	GluK1, 2F34	antagonist
LY466195	7.31	GluK1, 2QS4	antagonist
1^a	5.53		

^aLow energy conformation located by performing a stochastic conformational search (for details, see Methods).

Results and Discussion

From a drug design point of view, it is of the essence to distinguish between competitive and noncompetitive antagonists. While the chemical scaffold and binding site of noncompetitive antagonists may vary extensively, the chemical diversity of competitive antagonists is constrained by the nature of the orthosteric binding pocket. An analysis of reported competitive AMPA/KA receptor antagonists which comprise an α -amino acid moiety (Table 1) shows that such ligands are characterized by a longer distance between the α -carbon and the distal acidic functional group, as compared to reported agonists (10). This common structural feature prevents the bringing together of domain 1 (D1) and domain 2 (D2) of the ligand binding domain (LBD) (Figure 1), a biostructural reorganization which is essential for AMPA/KA receptor activation (calcium channel opening) (11–13).

Depending on the chemical nature of the antagonist, the KA receptor may be captured in diverse open states. For example, a superimposition study of X-ray structures of ATPO and LY466195 in GluK1 shows distinct spatial organization of the backbone and orientation of side chains of the D2 pocket (Figure 1). However, it remains to be understood if the distinct binding affinities of ATPO and LY466195 is a result thereof or simply due to disfavored ligand–receptor interactions.

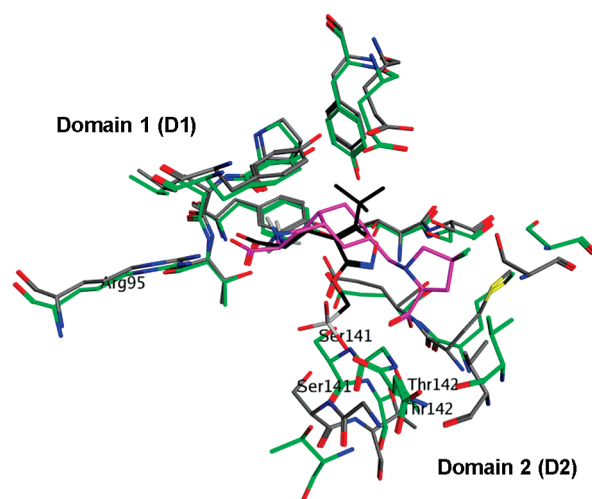


Figure 1. Superimposition of X-ray structures of the LBD of GluK1 cocrystallized with ATPO (black; 1VSO in type code) and with LY466195 (purple, 2QS4 in green) with an indication of the two binding domains D1 and D2. The two antagonists occupy distinct spatial positions with respect to their distal functional groups. Furthermore, the two residues important for the binding of the distal acid group, Ser141 and Thr142, are being forced out by ATPO by 2.85 Å and 1.55 Å, respectively.

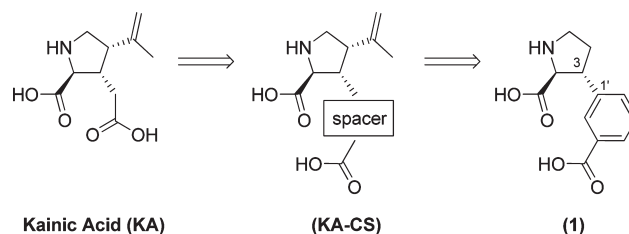


Figure 2. Chemical structures of iGluR agonist kainic acid (KA) and KA with the incorporation of a chemical spacer (KA-CS) leading to the rational design of potential iGluR antagonist **1**.

In our search for new lead structures for the development of KA antagonists which display a subtype selectivity profile, we looked toward the nonselective KA receptor agonist KA (Figure 2). We believed this compound served as an attractive starting point for the rational design of novel KA antagonists as it holds several possibilities for the introduction of substituents. By incorporation of a chemical spacer at the 3-position of the proline ring, the distance between the α -amino acid moiety and the distal carboxylic acid could be extended as desired. Several chemical spacers would do this; however, spatial orientation of the distal carboxylic acid group in the molecule's low-energy conformation, the possibility for future incorporation of substituents, and synthetic tractability pointed toward a meta-substituted phenyl ring as in **1** (Figure 2) as a first attempt. In this compound, the distance between the α -amino acid moiety and the distal carboxylic acid was calculated to be 5.53 Å.

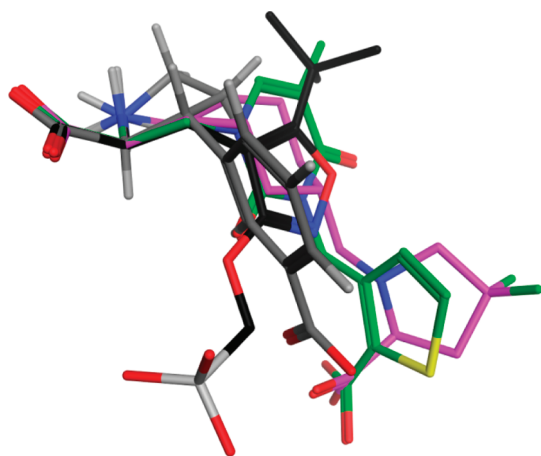


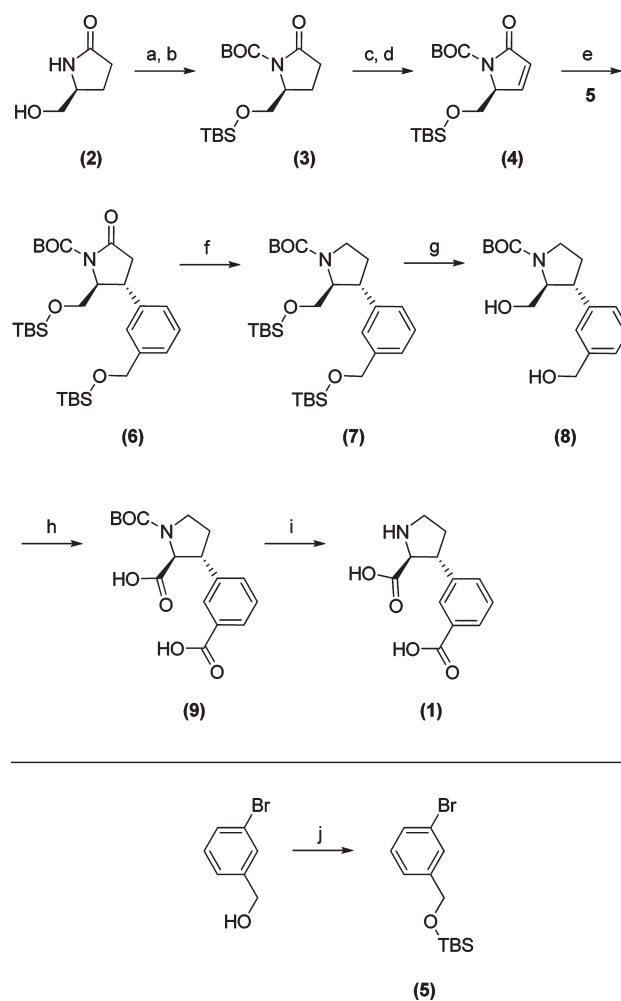
Figure 3. Superimposition of the low-energy conformation of **1** (type code) with the binding conformations of ATPO (black), UBP310 (green), and LY466195 (purple) obtained from X-ray crystal structures with PDB codes 1VSO, 2QS4, and 2F34, respectively.

A superimposition study of the low-energy conformation of **1** with the binding conformations of the KA receptor antagonists ATPO, UBP310, and LY466195 obtained from their respective KA receptor X-ray crystal structure was carried out (Figure 3). It shows that the distal carboxylic acid of **1** finds itself in between the distal functional groups of ATPO and UBP310/LY466195, being able to make essential interactions with Ser141 and Thr142 (GluK1 numbering). From the *in silico* study, it is also evident that **1** provides several options for the introduction of substituents into unexplored areas of the receptor which may be advantageous in subsequent work to improve potency and/or the subtype selectivity profile.

A retro synthetic analysis of **1** suggests (*S*)-pyroglutaminol (**2**) (Scheme 1) as the source of chirality for the α -amino acid. This stereogenic center may furthermore be used to direct the asymmetric introduction of the phenyl ring in the 3-position. It is well established that cuprate addition to enone **4** proceeds selectively with 2,3-*anti* stereo selectivity and that high yields may be obtained by the use of a method previously developed in our laboratories.

The synthesis commenced with *O*-TBS and *N*-BOC protection of **2** under standard conditions followed by the introduction of the double bond by α -selenation and oxidative elimination to give **4** (14). The cyano-Gilman cuprate of *O*-TBS-protected *m*-bromobenzylalcohol **5** was generated according to previously described methods (15, 16) and reacted with **4** to give the conjugated addition product **6**, in a stereoselective fashion as expected. Compound **6** was reduced using borane under reflux to give **7**. Removal of the TBS protecting groups by treatment with tetrabutylammonium fluoride (TBAF) gave free diol **8**. This deprotection step was performed

Scheme 1. Synthetic Pathway toward **1**^a



^a Reagents and conditions: (a) TBSCl, Et₃N, CH₂Cl₂; (b) BOC₂O, Et₃N, DMAP, CH₂Cl₂ (87% two steps); (c) LHMDs, THF, -78 °C, then PhSeCl; (d) H₂O₂, EtOAc, 0 °C to RT (65% two steps); (e) **5**, *t*-BuLi, CuCN, TMSCl, THF, -50 °C, then **4** (90%); (f) BH₃·THF, reflux, then NaOH, H₂O₂, 0 °C to rt (71%); (g) TBAF, THF, rt (94%); (h) RuCl₃, NaIO₄, H₂O, MeCN, EtOAc (75%); (i) HCl/dioxane, rt, then recrystallization from AcOH (44%); (j) TBSCl, imidazole, DMF (96%).

after the reduction of the endocarbonyl group in order to prevent undesired migration of the BOC group (17). Diol **8** was oxidized using Ru(III) in catalytic amount and periodate as the co-oxidant to give **9**, according to the modified Sharpless procedure (18). Finally, *N*-Boc deprotection of **9** using HCl in dioxane, followed by recrystallization from acetic acid gave the target compound **1**, as the HCl salt.

Pharmacological characterization of **1** commenced with binding studies at native AMPA, KA, and NMDA receptors from rat synaptosomes (Table 2). At AMPA and KA (predominantly the high KA affinity subtypes GluK4,5) receptors, **1** displayed medium-range micromolar affinity (51 and 22 μ M, respectively), whereas it showed a 3–9-fold higher affinity for the NMDA

Table 2. Binding Affinities of **1** at Native AMPA, KA, and NMDA Receptors (Rat Synaptosomes) and at Cloned Homomeric Rat GluA2 and GluK1-3 Receptors^a

	AMPA	KA	NMDA	GluA2	GluK1	GluK2	GluK3
	IC ₅₀	IC ₅₀	K _i	K _i	K _i	K _i	K _i
1	51 ± 10 ^b	22 ± 2 ^b	6.0 ± 0.5 ^b	67 ± 16 ^c	4.3 ± 0.4 ^c	> 100 ^c	8.1 ± 0.6 ^c
ATPO	16 ^f	> 100 ^f	> 100 ^f	60 ± 5 ^c	2.6 ± 0.4 ^c	> 100 ^c	> 1000
UBP310 ^d	--	--	--	> 100	0.010 ^e	> 100	0.023
LY466195 ^e	--	--	--	270	0.05	--	8.9

^aAll values are in μM . ^bMean values \pm SEM of three individual experiments. Radioligands used: AMPA, [³H]AMPA; KA, [³H]KA; NMDA, [³H]CGP 39653. ^cMean values \pm SEM of at least three experiments, conducted in triplicate at 12–16 drug concentrations. Radioligands used: GluA2, [³H]AMPA; GluK1–3, [³H](2*S*,4*R*)-4-methyl Glu (SYM2081). Hill coefficients were not different from unity. ^dK_b values for the inhibition of 100 μM glutamate-induced Ca²⁺ influx in HEK 293 cells expressing human homomeric AMPA or KA receptor subtypes (from refs 19 and 20). ^eIC₅₀ value for the inhibition of glutamate-evoked currents in HEK 293 cells expressing homomeric KA receptors. ^fFrom ref 21. ^gFrom ref 22. --: no data available.

Table 3. Functional Characterization of **1** Using TEVC Electrophysiology at Non-Desensitizing Mutant Homomeric GluK1-3^a

	GluK1 K _b	GluK2 K _b	GluK3 K _b
1 ^b	11.4 ± 2.8 (5)	> 300 (5)	275 ± 12 (6)
(<i>S</i>)-ATPO ^c	24	> 300	--
UBP310 ^b	0.019 ± 0.003 (6)	207 ± 34 (5)	0.394 ± 0.035 (9)
LY466195 ^d	0.024	--	--

^aAll values are in μM . ^bShown are the mean \pm SEM values from concentration–response curves conducted in duplicate at 7–9 antagonist concentrations. The number of experiments is indicated in parentheses. No agonistic activity was detected at 1 mM compound. ^cFrom refs 21 and 25. ^dFrom ref 22. --: no data available.

receptors (6.0 μM). To fully investigate its pharmacological profile at the KA receptors, **1** underwent binding affinity studies at cloned homomeric KA subtypes, GluK1–3 (Table 2). Here, **1** showed a clear selectivity profile for GluK1 and GluK3 over GluK2 (3 and 8 vs > 100 μM , respectively). In the same assay, the binding affinity of **1** was furthermore determined for AMPA receptor subtype GluA2, and the affinity was in agreement with the data obtained for native AMPA receptors (67 vs 51 μM , respectively).

To determine if **1** was capable of fully antagonizing KA receptor subtypes GluK1 and GluK3, two electrode voltage clamp (TEVC) electrophysiology was employed using homomeric nondesensitizing mutants of GluK1–3 (23). In this assay, **1** was shown to be a competitive full antagonist (efficacy = 0) at GluK1 and GluK3 with K_b values of 11.4 and 275 μM , respectively (Table 3 and Figure 4). The K_b value of **1** at GluK1 was within the expected range based on the binding affinity data, whereas K_b for GluK2 was too high to determine, which was anticipated from the radioligand binding data. The unexpected lower potency (34-fold) of **1** at the nondesensitizing GluK3 mutant compared to the binding affinity at wild-type GluK3 is not readily explained from a molecular or structural perspective. A reasonable explanation could be that the nondesensitizing GluK3 mutant is not well representative of the wild-type receptor,

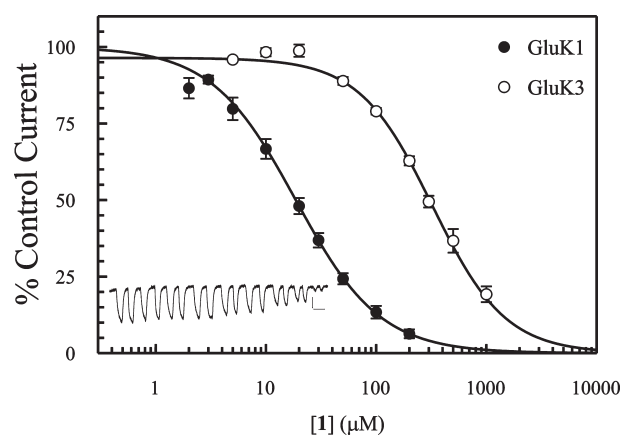


Figure 4. Inhibition of Glu responses by **1** at the nondesensitizing mutants of GluK1 and GluK3, expressed in *X. laevis* oocytes and measured by TEVC electrophysiology. Shown are the pooled data normalized to the control response in the absence of antagonist from 5 to 6 experiments conducted in duplicate. GluK1, Glu = 100 μM , IC₅₀ = 18.6 μM ; GluK3, Glu = 5 mM, IC₅₀ = 323 μM . Inset: traces from one oocyte expressing the GluK3 mutant. Stimulations in duplicate at increasing concentrations of **1** (in μM): 0, 5, 10, 20, 50, 100, 200, 300, 1000; (*V*_h = −90 mV). Scale bars: 50 nA and 1 min.

because the disulfide linkage which prevents conformational change of the receptor into the desensitized state could also interfere with D1–D2 domain movements associated with ligand binding. As such, **1** may not have the same LBD contacts in the mutant receptor as it has in the wild-type receptor, leading to a possible loss of binding affinity. Notably, the competitive antagonist UBP310 also exhibited a 17-fold higher K_b value at the nondesensitizing GluK3 receptor (Table 3) compared to the K_b value at wild-type GluK3 (Table 2). Finally, the wild-type GluK3 subtype has been shown to exhibit atypical function as compared to that of wild-type GluK1,2 (24).

On the comparison of **1** with KA antagonists ATPO, UBP310, and LY466195, it is clear that the pharmacological profile of **1** resembles mostly the profile observed for ATPO (Table 3). This finding is not surprising given

the information obtained from the initial molecular modeling study. While UBP310 and LY466195 occupy very similar GluK1 LBD spaces and are both highly potent selective GluK1 antagonists, ATPO deviates in spatial orientation, domain closure, and side chain/backbone organization as well as the pharmacological profile (Figure 1). With **1** estimated to exhibit medicinal chemistry properties in between ATPO and UBP310/LY466195, it is not unexpected that **1** could turn out to be ATPO-like rather than UBP310/LY466195-like in its pharmacological profile.

Conclusions

We have discovered a new class of iGluR antagonists by the rational design and synthesis of **1**. The compound was synthesized by a stereoselective approach in 10 steps from commercially available starting materials with the overall yield of 11%. The binding affinity profile reveals that **1** is fully selective for iGluRs, with no affinity for the mGluRs ($> 1000 \mu\text{M}$) (26). In more detail, **1** displayed a 3–9-fold higher affinity for native NMDA receptors over that of AMPA and KA receptors. Furthermore, affinity studies at cloned homomeric AMPA and KA subtypes revealed that **1** has low micromolar affinity for GluK1 with a > 20 fold selectivity over that of GluK2,3. Functional characterization of **1** in a TEVC electrophysiological assay using nondesensitizing homomeric mutants of GluK1–3 showed that **1** is a competitive full antagonist at GluK1 and GluK3. In all, **1** serves as a promising lead structure for the discovery of iGluR antagonists with novel subtype selectivity profiles. This is due to its broad but selective binding affinity profile for the iGluRs and its chemical scaffold, which allows for the introduction of substituents in diverse positions.

Methods

Chemistry

All reactions involving air- and moisture-sensitive reagents were performed in flame-dried glassware and under a nitrogen atmosphere using syringe–septum cap techniques. All reagents and solvents were purchased from Sigma-Aldrich and used without further purification unless otherwise specified. THF was distilled from Na/benzophenone under a nitrogen atmosphere prior to use. Et₂O was dried with and stored over Na-thread. DMF, CH₂Cl₂, and dioxane were dried by storing over molecular sieves (4 Å). Analytical thin-layer chromatography (TLC) was carried out using Merck Silica gel 60 F254 aluminum sheets. Compounds were detected as single spots on TLC plates and visualized using UV light (254 or 366 nm) and KMnO₄ or ninhydrin. Merck silica gel (35–70 mesh) was used for flash chromatography. Melting points were recorded on an SRS Optimelt apparatus and are uncorrected. ¹H NMR spectra were recorded on a 300 MHz Varian Mercury 300BB with a 5 mm ¹H probe. ¹³C NMR spectra were recorded on a 75 MHz Varian Gemini 2000BB spectrometer with a 5 mm

³¹P, ¹³C, ¹H, and ¹⁹F probe. NMR samples were prepared as CDCl₃ solutions using solvent peaks as a reference unless otherwise noted. The purity of tested compounds was determined by elementary analysis to be $> 95\%$.

(5S)-N-tert-Butoxycarbonyl-5-(tert-butyl)dimethylsilyloxy-methylpyrrolidin-2-one (3) (14). DMAP and Et₃N were used instead of imidazole. CH₂Cl₂ was used as the solvent instead of DMF. Yield 87%; ¹H NMR δ 4.17 (m, 1H), 3.92 (dd, 1H, $J = 10$ and 4 Hz), 3.69 (dd, 1H, $J = 10$ and 2 Hz), 2.72 (dt, $J = 17$ and 10 Hz), 2.38 (qd, $J = 17$, 9, and 2 Hz), 2.08 (m, 2H), 1.55 (s, 9H), 0.89 (s, 9H), 0.06 (s, 3H), 0.05 (s, 3H).

(5S)-N-tert-Butoxycarbonyl-5-(tert-butyl)dimethylsilyloxy-methyl-3-pyrrolidene-2-one (4) (14). EtOAc was used as the solvent instead of CH₂Cl₂. Yield 89%; ¹H NMR δ 7.21 (dd, 1H, $J = 6$ and 2 Hz), 6.07 (dd, 1H, $J = 6$ and 2 Hz), 4.56 (m, 1H), 4.11 (dd, 1H, $J = 10$ and 4 Hz), 3.67 (q, 1H, $J = 10$ and 7 Hz), 1.52 (s, 9H), 0.83 (s, 9H), 0.01 (s, 3H), 0.00 (s, 3H).

3-Bromo-[(tert-butyl)dimethylsilyloxy-methyl]benzene (5). Prepared according to the literature procedure in ref 27.

(4R,5S)-N-(tert-Butoxycarbonyl)-5-(((tert-butyl)dimethylsilyloxy)methyl)-4-(3-(((tert-butyl)dimethylsilyloxy)methyl)-phenyl)-pyrrolidin-2-one (6). To a solution of **5** (1.86 g, 6.50 mmol) in dry THF (22 mL) at -78°C was added *tert*-BuLi (7.65 mL, 1.7 M in pentane, 13.0 mmol). After stirring for 15 min, a suspension of CuCN (295 mg, 3.25 mmol) in dry THF (2 mL) was added, and the reaction mixture allowed to warm up to -50°C by removing dry ice and adding acetone (clear solution). After 5 min, the flask was recooled to -78°C , and **4** (847 mg, 2.6 mmol) dissolved in dry THF (2.0 mL) was added followed by TMSCl (0.85 mL, 6.50 mmol). The reaction mixture was allowed to warm up to -50°C and stirred at this temperature for 1 h. The reaction was quenched with sat. NH₄Cl and extracted with EtOAc. The organic layer was washed with brine, dried (MgSO₄), and concentrated. Purification of the crude product by flash chromatography (heptane, 1.5% EtOAc, $R_f = 0.24$) gave **7** as a white solid (1.24 g, 90%): mp = 68–69 °C; $[\alpha]_D^{24}{}_{589} = -42.85$ ($c = 0.49$, CH₂Cl₂); ¹H NMR δ 7.26 (m, 2H), 7.11 (br s, 1H), 7.05 (br d, 1H, $J = 7$ Hz), 4.71 (s, 2H), 4.06 (p, 1H, $J = 4$ and 2 Hz), 3.99 (dd, 1H, $J = 10$ and 4 Hz), 3.78 (dd, 1H, $J = 10$ and 2 Hz), 3.44 (dt, 1H, $J = 10$, 3, and 2 Hz), 3.13 (q, 1H, $J = 18$ and 10 Hz), 2.53 (dd, 1H, $J = 18$ and 3 Hz), 1.52 (s, 9H), 0.94 (s, 9H), 0.91 (s, 9H), 0.10 (s, 6H), 0.08 (s, 3H), 0.07 (s, 3H); ¹³C NMR δ 174.28, 150.00, 144.34, 142.44, 129.14, 125.02, 124.24, 83.16, 66.90, 64.99, 63.82, 40.16, 38.90, 28.25, 26.13, 26.03, -5.05 .

(2S,3R)-N-(tert-Butoxycarbonyl)-2-(((tert-butyl)dimethylsilyloxy)methyl)-3-(3-(((tert-butyl)dimethylsilyloxy)methyl)-phenyl)-pyrrolidine (7). To a solution of **6** (500 mg, 0.938 mmol) in dry THF (4 mL) was added a solution of borane (5.63 mL, 5.63 mmol, 1 M in THF), and the solution was stirred under reflux for 20 h. The flask was then cooled to 0°C , and 11.5 mL of THF was added. H₂O (0.5 mL) was then added carefully, followed by NaOH (7.60 mL, 2 N) and H₂O₂ (2.35 mL, 35 w/w%). The reaction mixture was then stirred at RT for 1 h and quenched with sat. NaHCO₃. The aqueous phase was extracted with EtOAc, and the collective organic layers were washed with brine, dried (MgSO₄), and concentrated. Purification of the crude product by flash chromatography

(heptane, 5% EtOAc, $R_f = 0.23$) gave **7** as a colorless oil (345 mg, 71%). $[\alpha]^{24}_{589} = +2.34$ ($c = 0.76$, CH_2Cl_2); ^1H NMR δ 7.22 (m, 1H), 7.13 (br d, 2H, $J = 7$ Hz), 7.03 (br t, 1H, $J = 7$ Hz), 4.67 (s, 2H), 4.00 – 3.45 (m, 5H), 3.29 (m, 1H), 2.19 (m, 1 Hz), 1.86 (m, 1H), 1.44 (s, 9H), 1.44 (s, 9H), 0.90 (s, 9H), 0.85 (s, 9H), 0.06 (s, 6H), 0.00 (s, 6H); ^{13}C NMR δ 154.41, 144.01, 143.54, 141.83, 128.63, 126.04, 125.13, 124.41, 79.55, 79.18, 65.74, 65.60, 65.15, 47.22, 46.64, 32.89, 32.05, 28.75, 26.15, –5.04, –5.20.

(2S,3R)-N-(tert-Butoxycarbonyl)-2-(hydroxymethyl)-3-(3-(hydroxymethyl)phenyl)-pyrrolidine (8). To a solution of **7** (795 mg, 1.53 mmol) in dry THF (13 mL) was added tetrabutylammonium fluoride (4.60 mL, 4.60 mmol, 1 M in THF). The reaction mixture was stirred for 1 h, then quenched with 1/2 sat. NaHCO_3 . The aqueous phase was extracted with EtOAc and the collective organic layers washed with brine, dried (MgSO_4), and concentrated. Purification of the crude product by flash chromatography (heptane/EtOAc 2:3, $R_f = 0.23$) gave **8** as a colorless oil (417 mg, 94%). $[\alpha]^{24}_{589} = -11.52$ ($c = 0.59$, CH_2Cl_2); ^1H NMR (d -DMSO) δ 7.25 (br t, 1H, $J = 7$ Hz), 7.14 (br d, 2H, $J = 7$ Hz), 7.04 (br d, 1H, $J = 7$ Hz), 5.16 (t, 1H, $J = 5$ Hz), 4.86 (br t, 1H, $J = 5$ Hz), 4.48 (br d, 2H, $J = 6$ Hz), 3.65 (br d, 1H, $J = 21$ Hz), 3.48 (m, 3H), 3.25 (m, 1H); 2.21 (m, 1H), 1.83 (m, 1H), 1.41 (s, 9H); ^{13}C NMR (CDCl_3) δ 156.89, 141.67, 141.04, 129.03, 128.32, 127.04, 126.26, 125.82, 80.70, 67.15, 65.99, 65.16, 47.26, 33.06, 28.60.

(2S,3R)-N-(tert-Butoxycarbonyl)-3-(3-(carboxyphenyl)-pyrrolidine-2-carboxylic acid (9). To **8** (532 mg, 1.83 mmol) dissolved in MeCN (13.0 mL) and EtOAc (13.0 mL) was added a solution of $\text{RuCl}_3 \cdot \text{H}_2\text{O}$ (7.7 mg, 0.034 mmol) and NaIO_4 (3.22 g, 15.05 mmol) in H_2O (23.0 mL). The reaction mixture was stirred for 1 h, then filtered on filter paper, and the filter cake washed with EtOAc. The aqueous phase was extracted with EtOAc and the collective organic layers washed with brine, dried (MgSO_4), and concentrated. Purification of the crude product by flash chromatography (heptane/EtOAc 2:3, 2% AcOH, $R_f = 0.32$) gave **9** as a white solid (444 mg, 75%), mp = 106–109 °C $[\alpha]^{24}_{589} = +53.03$ ($c = 0.69$, MeOH); ^1H NMR (CD_3OD) δ 7.93 (m, 2H), 7.52 (m, 2H), 7.44 (m, 1H), 7.15 (m, 1H), 4.24 (dd, 1H, $J = 22$ and 6 Hz), 3.69 (m, 1H), 3.55 (m, 2H), 2.36 (m, 1H), 2.09 (m, 1H), 1.53 (s, 9H); ^{13}C NMR (CD_3OD , two conformers) δ 175.91, 175.67, 169.60, 156.07, 155.67, 143.11, 142.51, 132.94, 132.80, 132.44, 130.03, 129.69, 129.60, 129.46, 129.32, 81.99, 81.63, 67.36, 66.87, 51.13, 50.07, 47.42, 47.17, 33.96, 33.44, 28.79, 28.60.

(2S,3R)-3-(3-(Carboxyphenyl)-pyrrolidine-2-carboxylic acid (1). To **9** (416 mg, 1.29 mmol) in 1,4-dioxane (2 mL) at 0 °C was added HCl(g) /1,4-dioxane (3.88 mL, 15.5 mmol, 4.0 M). The reaction mixture was stirred at RT for 1 h then concentrated. The solid was triturated with freezing cold diethyl ether to give the HCl salt of **1** as a white solid. Recrystallization from glacial acetic acid gave the HCl salt of **1** as white crystals (146 mg, 44%); TLC (MeOH/AcOH/EtOAc 1:1:3) $R_f = 0.24$; mp = 190–193 °C; $[\alpha]^{24}_{589} = +63.71$ ($c = 0.62$, MeOH); ^1H NMR (CD_3OD , TMS standard ref.) δ 8.05 (br t, 1H, $J = 3$ and 2 Hz), 7.96 (dt, 1H, $J = 8$ and 1 Hz), 7.63 (dt, 1H, $J = 8$ and 1 Hz), 7.49 (t, 1H, $J = 15$ and 8 Hz), 4.41 (d, 1H, $J = 9$ Hz), 3.67 (m, 2H), 3.47 (m, 1H), 2.57 (m, 1H), 2.25 (m, 1H); ^{13}C NMR (CD_3OD) δ 170.41, 169.19, 140.55, 133.20, 132.55,

130.10, 130.03, 129.77, 65.98, 49.59 (approximated from D_2O spectrum.), 47.00, 34.78. Elem. anal. calcd. for $\text{C}_{12}\text{H}_{14}\text{ClNO}_4$, C, 53.05; H, 5.19; N, 5.16; found, C, 52.68; H, 5.03; N, 4.97.

Molecular Modeling

The modeling study was performed using the software package MOE (Molecular Operating Environment, v2009.10, Chemical Computing Group, 2009) using the built-in mmff94x forcefield and the GB/SA continuum solvent model. The compound was submitted to a stochastic conformational search, and with respect to its global minimum (ΔG in kcal/mol), returned conformations above +7 kcal/mol were discarded. The γ -carboxylate group was protonated prior to execution of the conformational search, as this gave a larger and thus more reliable number of output conformations. The superimposition of ligands was carried out using the built-in function in MOE, by fitting the ammonium group and the two carboxylate groups.

Pharmacology

Native Receptor Binding Assays. Affinities for native AMPA, KA, and NMDA receptors in rat cortical synaptosomes were determined using 5 nM (*RS*)- ^3H AMPA (55.5 Ci/mmol) (**28**), 5 nM ^3H KA (58.0 Ci/mmol) (**29**), and 2 nM ^3H CGP 39653 ($K_d = 6$ nM, 50.0 Ci/mmol) (**30**), respectively, with minor modifications as previously described (**31**, **32**).

Recombinant Receptor Binding Assays. *Sf9* cells were cultured and infected with recombinant baculovirus of cloned rat GluA2(*R*)_o or GluK1–3 and membranes prepared and used for binding as previously detailed (**33**, **34**). The binding affinity of **1** was determined from competition experiments with 2–5 nM (*RS*)- ^3H AMPA (42.1 Ci/mmol; PerkinElmer, Waltham, MA) at GluA2(*R*)_o or 1–5 nM ^3H SYM2081 (40 Ci/mmol; ARC, St. Louis, MO) at GluK1(*Q*)_{1b}, GluK2-*(V,C,R)*_a, and GluK3_a. The italic letters in parentheses indicate the RNA-edited isoforms of the subunits used. The IC_{50} , Hill coefficient, and K_i values for **1** were evaluated as previously described (**35**).

TEVC Electrophysiology. *X. laevis* oocytes were collected, prepared, injected, and maintained as previously described (**36**). TEVC electrophysiology was also carried out as previously described (**36**) on nondesensitizing mutants of GluK1–3 (**23**). Antagonist concentration–response data were fit to the logistic equation: $I = I_{\text{max}}/(1 + (10^{(\log[B] - \log \text{IC}_{50})n_H}))$, where I is the agonist-evoked current, $[B]$ is the antagonist concentration, I_{max} is the control response in the absence of antagonist, IC_{50} is the concentration of the antagonist giving 50% inhibition, and n_H is the Hill coefficient. (*S*)-Glutamate was used as the agonist (100 μM at GluK1 and 2; 5 mM at GluK3; $\text{EC}_{50} = 83.5$ μM , 108 μM , and 9.03 mM, respectively). K_b values were calculated from the IC_{50} value using the modified Cheng–Prusoff equation (**37**).

Author Information

Corresponding Author

*Phone: +45 35336244. Fax: +45 35336041. E-mail: lebu@farma.ku.dk.

Funding Sources

We thank Carlsberg Foundation, Lundbeck Foundation, and GluTarget for financial support.

Abbreviations

CNS, central nervous system; D1, domain 1 of the LBD; D2, domain 2 of the LBD; KA, kainic acid; Glu, glutamate; LBD, ligand binding domain; SAR, structure–activity relationship; TBAF, tetrabutylammonium fluoride; TEVC, two electrode voltage clamp.

References

1. Kaczor, A. A., and Matosiuk, D. (2010) Molecular structure of ionotropic glutamate receptors. *Curr. Med. Chem.* *17*, 2608–2635.
2. Chen, P. E., and Wyllie, D. J. A. (2006) Pharmacological insights obtained from structure-function studies of ionotropic glutamate receptors. *Br. J. Pharmacol.* *147*, 839–853.
3. Ferraguti, F., and Shigemoto, R. (2006) Metabotropic glutamate receptors. *Cell Tissue Res.* *326*, 483–504.
4. Bartolotto, and Clarke, Z. A. (1999) Kainate receptors are involved in synaptic plasticity. *Nature* *402*, 297.
5. Mellor, J. R. (2006) Synaptic plasticity of kainate receptors. *Biochem. Soc. Trans.* *34*, 949–951.
6. Bloss, E. B., and Hunter, R. G. (2010) Hippocampal kainate receptors. *Vitam. Horm.* *82*, 167–184.
7. Nistico, R., Dargan, S., Fitzjohn, S. M., Lodge, D., Jane, D. E., Collingridge, G. L., and Bartolotto, Z. A. (2009) GLUK1 receptor antagonists and hippocampal mossy fiber function. *Int. Rev. Neurobiol.* *85*, 13–27.
8. Lau, A., and Tymianski, M. (2010) Glutamate receptors, neurotoxicity and neurodegeneration. *Pflugers Arch.* *460*, 525–542.
9. Jane, D. E., Lodge, D., and Collingridge, G. L. (2009) Kainate receptors: pharmacology, function and therapeutic potential. *Neuropharmacology* *56*, 90–113.
10. Bunch, L., and Krosggaard-Larsen, P. (2009) Subtype selective kainic acid receptor agonists: discovery and approaches to rational design. *Med. Res. Rev.* *29*, 3–28.
11. Gill, A., Birdsey-Benson, A., Jones, B. L., Henderson, L. P., and Madden, D. R. (2008) Correlating AMPA receptor activation and cleft closure across subunits: crystal structures of the GluR4 ligand-binding domain in complex with full and partial agonists. *Biochemistry* *47*, 13831–13841.
12. Armstrong, N., and Gouaux, E. (2000) Mechanisms for activation and antagonism of an AMPA-sensitive glutamate receptor: Crystal structures of the GluR2 ligand binding core. *Neuron* *28*, 165–181.
13. Mayer, M. L., Ghosal, A., Dolman, N. P., and Jane, D. E. (2006) Crystal structures of the kainate receptor GluR5 ligand binding core dimer with novel GluR5-selective antagonists. *J. Neurosci.* *26*, 2852–2861.
14. Acevedo, C. M., Kogut, E. F., and Lipton, M. A. (2001) Synthesis and analysis of the sterically constrained L-glutamine analogues (3S,4R)-3,4-dimethyl-L-glutamine and (3S,4R)-3,4-dimethyl-L-pyroglutamic acid. *Tetrahedron* *57*, 6353–6359.
15. Bunch, L., Krosggaard-Larsen, P., and Madsen, U. (2002) Mixed cyano-gilman cuprates: advances in conjugate addition to alpha,beta-unsaturated pyroglutaminol. *Synthesis* 31–33.
16. Bunch, L., Nielsen, B., Jensen, A. A., and Brauner-Osborne, H. (2006) Rational design and enantioselective synthesis of (1R,4S,5R,6S)-3-azabicyclo[3.3.0]octane-4,6-dicarboxylic acid - A novel inhibitor at human glutamate transporter subtypes 1, 2, and 3. *J. Med. Chem.* *49*, 172–178.
17. Bunch, L., Norrby, P. O., Frydenvang, K., Krosggaard-Larsen, P., and Madsen, U. (2001) Unprecedented migration of N-alkoxycarbonyl groups in protected pyroglutaminol. *Org. Lett.* *3*, 433–435.
18. Carlsen, P. H. J., Katsuki, T., Martin, V. S., and Sharpless, K. B. (1981) A greatly improved procedure for ruthenium tetraoxide catalyzed oxidations of organic-compounds. *J. Org. Chem.* *46*, 3936–3938.
19. Dolman, N. P., More, J. C. A., Alt, A., Knauss, J. L., PentikÄ-inen, O. T., Glasser, C. R., Bleakman, D., Mayer, M. L., Collingridge, G. L., and Jane, D. E. (2007) Synthesis and pharmacological characterization of N3-substituted willardiine derivatives: role of the substituent at the 5-position of the uracil ring in the development of highly potent and selective GLUK5 kainate receptor antagonists. *J. Med. Chem.* *50*, 1558–1570.
20. Perrais, D., Pinheiro, P. S., Jane, D. E., and Mülle, C. (2009) Antagonism of recombinant and native GluK3-containing kainate receptors. *Neuropharmacology* *56*, 131–140.
21. Moller, E. H., Egebjerg, J., Brehm, L., Stensbol, T. B., Johansen, T. N., Madsen, U., and Krosggaard-Larsen, P. (1999) Resolution, absolute stereochemistry, and enantio-pharmacology of the GluR1–4 and GluR5 antagonist 2-amino-3-[5-tert-butyl-3-(phosphonomethoxy)-4-isoxazolyl]-propionic acid. *Chirality* *11*, 752–759.
22. Weiss, B., Alt, A., Ogden, A. M., Gates, M., Dieckman, D. K., Clemens-Smith, A., Ho, K. H., Jarvie, K., Rizkalla, G., Wright, R. A., Calligaro, D. O., Schoepp, D., Mattiuz, E. L., Stratford, R. E., Johnson, B., Salhoff, C., Katofiasc, M., Phebus, L. A., Schenck, K., Cohen, M., Filla, S. A., Ornstein, P. L., Johnson, K. W., and Bleakman, D. (2006) Pharmacological characterization of the competitive GLU-(K5) receptor antagonist decahydroisoquinoline LY466195 in vitro and in vivo. *J. Pharmacol. Exp. Ther.* *318*, 772–781.
23. Weston, M. C., Schuck, P., Ghosal, A., Rosenmund, C., and Mayer, M. L. (2006) Conformational restriction blocks glutamate receptor desensitization. *Nat. Struct. Mol. Biol.* *13*, 1120–1127.
24. Perrais, D., Coussen, F., and Mülle, C. (2009) Atypical functional properties of GluK3-containing kainate receptors. *J. Neurosci.* *29*, 15499–15510.
25. Wahl, P., Anker, C., Traynelis, S. F., Egebjerg, J., Rasmussen, J. S., Krosggaard-Larsen, P., and Madsen, U. (1998) Antagonist properties of a phosphono isoxazole amino acid at glutamate R1–4 (R,S)-2-amino-3-(3-hydroxy-5-methyl-4-isoxazolyl)propionic acid receptor subtypes. *Mol. Pharmacol.* *53*, 590–596.
26. Micheli, F., Di Fabio, R., and Marchioro, C. (1999) Asymmetric synthesis of some substituted-3-phenyl prolines. *Farmaco* *54*, 461–464.
27. Doucet-Personeni, C., Bentley, P. D., Fletcher, R. J., Kinkaid, A., Kryger, G., Pirard, B., Taylor, A., Taylor, R.,

Taylor, J., Viner, R., Silman, I., Sussman, J. L., Greenblatt, H. M., and Lewis, T. (2001) A structure-based design approach to the development of novel, reversible AChE inhibitors. *J. Med. Chem.* *44*, 3203–3215.

28. Honore, T., and Nielsen, M. (1985) Complex structure of quisqualate-sensitive glutamate receptors in rat cortex. *Neurosci. Lett.* *54*, 27–32.

29. Braitman, D. J., and Coyle, J. T. (1987) Inhibition of [H-3] kainic acid receptor-binding by divalent-cations correlates with ion affinity for the calcium-channel. *Neuropharmacology* *26*, 1247–1251.

30. Sills, M. A., Fagg, G., Pozza, M., Angst, C., Brundish, D. E., Hurt, S. D., Wilusz, E. J., and Williams, M. (1991) [H-3] Cgp-39653 - A new N-methyl-D-aspartate antagonist radioligand with low nanomolar affinity in rat-brain. *Eur. J. Pharmacol.* *192*, 19–24.

31. Hermit, M. B., Greenwood, J. R., Nielsen, B., Bunch, L., Jorgensen, C. G., Vestergaard, H. T., Stensbol, T. B., Sanchez, C., Krosgaard-Larsen, P., Madsen, U., and Bräuner-Osborne, H. (2004) Ibotenic acid and thioibotenic acid: a remarkable difference in activity at group III metabotropic glutamate receptors. *Eur. J. Pharmacol.* *486*, 241–250.

32. Clausen, R. P., Hansen, K. B., Cali, P., Nielsen, B., Greenwood, J. R., Begtrup, M., Egebjerg, J., and Brauner-Osborne, H. (2004) The respective N-hydroxypyrazole analogues of the classical glutamate receptor ligands ibotenic acid and (RS)-2-amino-2-(3-hydroxy-5-methyl-4-isoxazolyl)acetic acid. *Eur. J. Pharmacol.* *499*, 35–44.

33. Vogensen, S. B., Clausen, R. P., Greenwood, J. R., Johansen, T. N., Pickering, D. S., Nielsen, B., Ebert, B., and Krosgaard-Larsen, P. (2005) Convergent synthesis and pharmacology of substituted tetrazolyl-2-amino-3-(3-hydroxy-5-methyl-4-isoxazolyl)propionic acid analogues. *J. Med. Chem.* *48*, 3438–3442.

34. Sagot, E., Pickering, D. S., Pu, X., Umberti, M., Stensbøl, T. B., Nielsen, B., Chapelet, M., Bolte, J., Gefflaut, T., and Bunch, L. (2008) Chemo-enzymatic synthesis of a series of 2,4-syn-functionalized (S)-glutamate analogues: new insight into the structure-activity-relation of ionotropic glutamate receptor subtypes 5, 6 and 7. *J. Med. Chem.* *51*, 4093–4103.

35. Nielsen, B. S., Banke, T. G., Schousboe, A., and Pickering, D. S. (1998) Pharmacological properties of homomeric and heteromeric GluR1(o) and GluR3(o) receptors. *Eur. J. Pharmacol.* *360*, 227–238.

36. Greenwood, J. R., Mewett, K. N., Allan, R. D., Martin, B. O., and Pickering, D. S. (2006) 3-hydroxypyridazine 1-oxides as carboxylate bioisosteres: a new series of subtype-selective AMPA receptor agonists. *Neuropharmacology* *51*, 52–59.

37. Leff, P., and Dougall, I. G. (1993) Further concerns over Cheng-Prusoff analysis. *Trends Pharmacol. Sci.* *14*, 110–112.